# Heat and Mass Transfer at interfaces between solid surfaces and Non-Newtonian Fluids

**A. S. Moita**
IN+ - Center for Innovation, Technology and Policy Research, Instituto Superior Técnico, Universidade de Lisboa, Lisbon, Portugal
Email: anamoita@dem.ist.utl.pt

## Abstract

The present paper reviews the fluid dynamic and heat transfer mechanisms occurring as Newtonian and non-Newtonian droplets interact with rigid surfaces. Several approaches on the constitutive models and governing parameters are discussed and alternative methods to model the spreading of non-Newtonian droplets are proposed, particularly for shear-thinning droplets. In this process, the results presented here evidence the importance of an adequate scaling of the dissipative term which must take into account the particular morphological features introduced by the different rheological properties of the non-Newtonian fluids.

The effect of various parameters is also addressed in an experimental study. Emphasis is given on the interaction of the droplets over enhanced surfaces, as a way to promote controllable fluid motion and heat transfer processes.

## 1 Introduction

Unlike Newtonian fluids, for which the stress tensor is a linear function of the velocity gradient and therefore the viscosity remains constant, regardless of the shear rate, in non-Newtonian fluids, the stress tensor is a generic function of the velocity gradient and of its derivatives. Usually, non-Newtonian fluids are categorized in three main groups: i) Power-law (or Ostwald-De Waele) fluids, ii) Yield-stress fluids and iii) Viscoelastic fluids.

Power law fluids are the simplest type of non-Newtonian Fluids [1], for which the viscosity μ is simply related to the shear rate $\dot{\gamma}$ by:

$$\mu = K \dot{\gamma}^{n-1} \tag{1}$$

Here $K$ and n are constants of empirical nature. $K$ is called as consistency coefficient and describes the fluid viscosity at low shear rates and matches with the Newtonian viscosity for $n$=0. The power-law index $n$ determines the behaviour of the fluid. Hence, the fluids are shear-thinning when $n$<1 (i.e. the viscosity decreases with the shear rate) and shear thickening for $n$>1. From the physical-chemical point of view, the shear thinning behaviour can be explained by the breakdown

of the structure formed by interacting particles within the fluid, while the shear-thickening is often related to flow-induced jamming [1,2].

As a constitutive model, the Ostwald-De Waele equation is not a practical approach, as it implies that the viscosity will change indefinitely for any values of the shear rate. Instead, in the constitutive Cross model [3] there are characteristically two plateaus of Newtonian behaviour in the viscosity curve: $\mu_0$, where the shear-rate is extremely low and $\mu_\infty$ where the shear-rate is extremely high [4]. The viscosity in- or decreases monotonously in between those limits, as illustrated in Figure 1, for a shear-thinning fluid.

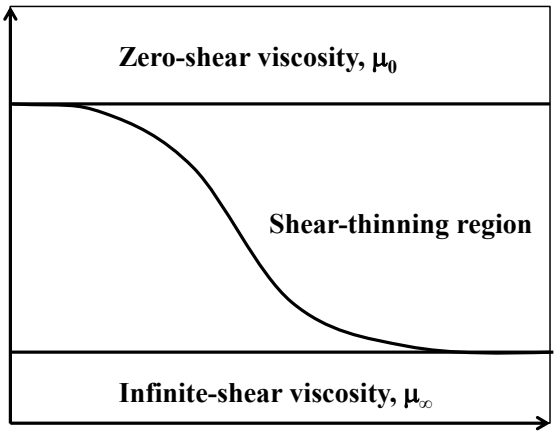


**Figure 1: Typical viscosity curve of a shear-thinning fluid with the Newtonian plateaus $\mu_0$ and $\mu_\infty$.**

The Cross model is given by:

$$\frac{\mu-\mu_\infty}{\mu_0-\mu_\infty}=\frac{1}{1+(C\dot{\gamma})^{1-n}} \tag{2}$$

while the Carreau model [5] suggests a slight modification to the power index:

$$\frac{\mu-\mu_\infty}{\mu_0-\mu_\infty}=\frac{1}{\left[1+(C\dot{\gamma})^{a}\right]^{(1-n)/a}} \tag{3}$$

A variant of this model is the Carreau-Yasuda equation, for which *a=2*. Alternatively, Ellis constitutive model proposes a different approach, also based on the Cross model, by setting $\mu_\infty=0$:

$$\frac{\mu_0}{\mu}=1+\left(\frac{\tau}{\tau_1/2}\right)^{n-1} \tag{4}$$

Here, $\tau$ is the applied shear stress and $\tau_1/2$ is the shear stress at which $\mu$ is exactly half of the zero-shear viscosity value [1].

Viscoplastic (or yield-stress) fluids are quite important in numerous industrial applications dealing with suspensions, paints, various polymer solutions, muds, cosmetic creams foams and emulsions, among others. Such fluids only flow when the applied stresses overcome a critical value

(the yield stress). For applied stresses lower than the yield stress, these fluids behave like elastic solids.

The discussion on the definition on yield-stress behaviour for a fluid instead of a solid is still a topic for discussion nowadays [1]. More extensive reviews on this subject can be found for instance in [6-9].

In terms of constitutive models, a simple model was proposed by Bingham [10] and introduces the shear stress component as a linear function of the velocity gradient. This intercepts at a critical value $\tau_c$ corresponding to the threshold yield point. An enhancement of the Bingham model was introduced by Herschel-Bulkley [11]:

$$\tau = G\gamma \qquad \text{for } \tau \leq \tau_c \tag{5.1}$$

$$\tau = \tau_c + K\dot{\gamma}^n \qquad \text{for } \tau > \tau_c \tag{5.2}$$

being G the shear modulus and $\gamma$ the shear deformation. Alternatively, Casson proposes [9 69]

$$\tau^{1/2} = \tau_c^{1/2} + (\mu\dot{\gamma}) \qquad \text{for } \tau > \tau_c \tag{6}$$

The approaches of [10] and [11] are very similar, except for higher shear rates, at which the model of [10] provides lower values of stress. Both approaches consider an abrupt transition from the elastic to the fluid regime (a specific point of $\tau_c$), which is a problem for determining numerical solutions, given that there is a first-order discontinuity in the shear stress derivative with respect to the shear rate. To solve this discontinuity Papanastasiou [12] proposes a smooth transition between the elastic and the fluid regime, given by equation:

$$\tau = \tau_c\left[1 + \exp(-B\dot{\gamma})\right] + C\dot{\gamma}^n \tag{7}$$

where B is a material-dependent constant. As in most real systems, such abrupt transitions are rarely observed so in this context, one may argue that Papanastasiou's model [12] provides a better description of real viscoplastic fluids.

Finally, in viscoelastic fluids (*e.g.* several polymer melts or solutions), part of the deformation energy is stored and released later, being the delay between energy storage and release related to a relaxation time. The main characteristic of the viscoelastic fluids is the occurrence of elastic stress effects, for sufficiently high shear rates. This characteristic leads to an anisotropic application of the normal forces (*e.g.* pressure) acting on liquid finite element, contrarily to what occurs in Newtonian fluids. Pioneering work introduced by Maxwell provides the basic constitutive model for linear viscoelastic fluids. A more elaborate model and probably the most popular is the Oldroyd-B model [8,9,13], which can be reviewed in detail in [1]. More recent constitutive models have been proposed for instance by Zhu *et al.* [14], to describe flow induced anisotropic behaviour of viscoelastic fluids.

Non-Newtonian fluid flows are present in a variety of situations. Droplet-wall interactions are a particularly interesting flow given its interest in numerous applications, such as coating, painting or printing. Bertola and Sefiane [15] suggest great potential in using non-Newtonian fluids in cooling applications. Fundamental and applied research have been developed within more than a century on droplet-wall interactions with Newtonian fluids, but studies with non-Newtonian droplets are still sparsely reported in the literature.

An increasingly interest on droplet-wall interactions of non-Newtonian liquids is also related to its relevance in various biological applications. For instance, droplet impacts of non-Newtonian preparations are the basic working principle of a method called cell printing. In this method various techniques similar to inkjet printing (*e.g.* Son and Kim [16]) are being used to deploy living cells on a substrate to create tissue, neural cells and possibly organs (*e.g.* [17-18]). In this case, great care is necessary as the cells are extremely sensitive to shear stresses and can be easily destroyed as the droplet impacts and spreads over the surface. Similar disruptive effects have been reported in the transport of DNA samples for several years [19]. Blood is a shear-thinning fluid whose behaviour is well characterized by Eq. (1). Modifications of the values of the consistency coefficient *K* and of the power-law index *n* are suggested to be correlated with leukemia [20]. Also, although human blood plasma has reported to depict majorly a Newtonian behaviour in shear, viscoelastic characteristics may be observed in elongational flows [21].

From the phenomenological point of view, droplet-wall interactions involving non-Newtonian fluids are also of major interest as they involve large special and temporal gradients, so the behaviour of a non-Newtonian droplet can be significantly different form that of a Newtonian one.

In line with this, the paper presented here focuses on the fluid dynamic and heat transfer processes occurring between non-Newtonian liquids and solid surfaces, with particular emphasis on droplet-wall interactions. Hence, following this introduction, section 2 briefly summarizes the dynamic behaviour of Newtonian droplets impacting on both cold and heated surfaces, relating the dynamic and the heat transfer behaviour for the latter case. In section 3, droplet-wall interactions are approached using non-Newtonian fluids. Particular emphasis is given here to spreading and (thermal) induced atomization phenomena.

## 2 Dynamic behaviour of Newtonian droplets impacting onto rigid surfaces

The dynamic behaviour of a droplet impacting on a rigid surface primarily depends on the forces acting on the droplet, namely inertial, viscous and surface tension forces. The magnitude of these forces can be related to the droplet initial diameter $D_0$, to the impact velocity $U_0$ and to the thermophysical properties of the fluid. Considering a dimensionless analysis, the most relevant dimensionless numbers, relating the magnitude of the aforementioned forces are the Reynolds number Re=inertial forces/viscous forces=$\rho D_0 U_0/\mu$, the Weber number We=inertial forces/surface tension forces= $\rho D_0 U_0^2/\sigma_{lv}$ and the Ohnesorge number Oh=surface tension forces/viscous forces = $(We)^{1/2}/Re$. Here $\rho$, $\mu$ and $\sigma_{lv}$ represent the density, the dynamic (Newtonian) viscosity and the surface tension of the liquid, respectively.

Additionally, the impact outcomes are also strongly dependent on the boundary conditions related to the interface (wettability) as well as to several surface properties (*e.g.* topography, which in turn affects the wettability, surface temperature and thermal properties). The presence of a liquid film over the surface also greatly affects the impact outcomes.

### 2.1 Droplet impacts onto cold surfaces

Starting with the simplest case possible, i.e. a Newtonian droplet impacting onto a cold surface, several phenomena can be identified. As argued in Moreira *et al.* [22] one may look at the

phenomena from the perspective of the variation of the impact energy or from the perspective of the characteristic time scale. Considering the variation of impact energy, three main phenomena can be readily identified, namely stick and spread, disintegration (often named "splash") and rebound. While rebound requires particular conditions at the surface/droplet interface to occur and may take tens or even hundreds of milliseconds to occur, stick and spread occur at low impact energy and take place in tens of milliseconds. A stagnation point is located at the impact region so, the flow spreads symmetrically and radially over the surface, forming a thin film called lamella. As the impact energy is slowly increased, the rim of the lamella can be disturbed and regular structures form called fingers. Once again, particular surface conditions (topography and wettability) may lead to the separation of these fingers and disruption of the lamella (Moita and Moreira [23]). The film extends until reaching a maximum diameter, resulting from the equilibrium between inertial, wetting and viscous forces. Then, given the excess of surface energy, the liquid tends to recoil back to the central region (impact region) and also here particular wetting and topographical conditions may promote the disruption of the lamella (the so-called receding break-up as identified by Rioboo *et al.* [24]. Further increasing the impact energy, the inertial forces promptly overcome surface tension and viscous effects thus promoting the disintegration of the droplet within the first micro-seconds after impact. This process is called "prompt splash" and is strongly promoted to occur at lower impact energy, for increased roughness amplitude. Once again, particular wetting conditions may also promote a different kind of "splash" also requiring high impact energy, although in this case, the phenomena is governed by aerodynamic forces (Moita and Moreira [23], Xu *et al.* [25], Jepsen *et al.* [26)] – the so-called "*corona splash*". It is worth noting that the term splash is often abusively used in the literature to determine any kind of droplet disintegration. However, care must be taken since, as shown in this brief description, there are dissimilar disintegration mechanisms, which depend on different impact energy values as well as on different interface conditions (wettability and surface topography) as extensively investigated by many authors such as Moita and Moreira [23], Rioboo *et al.* [24] and Xu *et al.* [25]. This is an issue of major importance when establishing the critical conditions for the occurrence of each of the aforementioned phenomena. For instance, most of the criteria establishing the limiting conditions for the occurrence of spreading or disintegration address only the "prompt splash".

A detailed description of each of these phenomena can be found for instance in the review of Yarin [27].

Additional complexity is added to the analysis when the surface is wetted by a liquid film (which can be for instance a previously impacted droplet). Here, the critical conditions for the occurrence of disintegration must be related to the ratio between the thickness of the film and the roughness amplitude of the surface, as the physical mechanism governing droplet disintegration is now related to a kinematic discontinuity occurring at the liquid film [28]. Exhaustive analysis of the disintegration mechanisms, the criteria for disintegration on both dry and wetted surfaces and the characterization of the resulting secondary droplets can be found in Moreira *et al.* [22].

In many of the practical applications referred in the Introduction, including cooling, the most relevant phenomenon is the spreading of the droplet over the surface. It is therefore relevant to present in more detail the physical processes governing this process.

## 2.2 Spreading of Newtonian droplets

Most contemporary semi-empirical models for the description of the spreading are based on a simple energy conservation equation (neglecting variations of the potential energy):

$$E_{Ki} + E_{Si} = E_{Kf} + E_{Sf} + E_{diss} \tag{8}$$

being $E_K$ and $E_S$ the kinetic and surface energy, respectively and $E_{diss}$ the energy dissipated by viscous effects. The subscripts *i* and *f* stand for the initial and final states, respectively.

The final state (*f*) is usually taken at the position where the diameter of the lamella is maximum, where $E_{diss}$ and $E_{Sf}$ can be easily determined [29]. Most of these models derive analytical expressions to predict the maximum spreading diameter, often made dimensionless with $D_0$ (the so-called spreading factor, $\beta=d(t)/D_0$).

Major differences between the various existing models lay in the assumptions regarding the shape of the lamella, the estimation of $E_{Kf}$ and $E_{diss}$ and the way to account for wettability effects.

The kinetic energy at the maximum extent of the lamella is often disregarded, which is not entirely correct, although it leads to good agreement with the experiments, probably because most are validated for impacts at small or moderate velocities [29]. Few exceptions have been observed, as for instance in the work of Roisman *et al.* [30]. Regarding the energy dissipation term, it can be determined by:

$$E_{diss} = \int_0^{t_2} \int_V \phi dV dt \approx \phi V t_2 \tag{9}$$

where $\phi = \mu\left(\partial U_i / \partial x_j + \partial U_j / \partial x_i\right)\partial U_i / \partial x_j$ is the dissipation function and $t_2$ is a known time period after impact, for which the effect of viscous dissipation is expected to be relevant. The viscous dissipation function is subsequently scaled based on different assumptions. For instance, Chandra and Avesidian [31] scale the viscous function with the impact velocity $U_0$ and with the thickness of the lamella *h*, which was determined by mass conservation, approximating the lamella to a flattened disk:

$$h = \frac{2}{3}\frac{D_0^3}{d_{max}^2} \tag{10}$$

Other authors proposed to use the boundary layer thickness $\delta$ as a scaling length, *e.g.* Pasandideh-Fard *et al.* [32] or Mao *et al.* [33], claiming that an overestimation of the maximum spreading diameter is obtained when *h* is used in the scaling. Hence, for instance, Pasandideh-Fard *et al.* [32] modified the model proposed by Chandra and Avedisian [31] by introducing the scaling with the boundary layer thickness, obtaining for the maximum spreading prediction, using the (dynamic) advancing contact angle $\theta_a$ to account for wetting effects:

$$\beta_{max} = \left( \frac{We + 12}{3.(1 - \cos\theta_a + 4.(We / Re^{1/2})} \right)^{1/2} \tag{11}$$

German & Bertola [34] performed an extensive review of different maximum spreading prediction models for Newtonian fluids and compared them with their own experimental results. The outcome of this analysis was a modified version of the model proposed by Mao *et al.* [33]:

$$\left[\frac{1}{4}.(1-\cos\theta_e)+\zeta.\frac{We^{0.83}}{Re^{\varphi}}\right].\beta_{max}^{3}-\left(\frac{We}{12}+1\right).\beta_{max}+\frac{2}{3}=0 \tag{12}$$

with: $\varphi = 0.45.Oh^{0.05}$ and $\xi = 0.07.We^{0.2}$ .

Besides replacing some other coefficients, [34] optimized the empirical power law exponent of the Reynolds number with a dependency of the Weber number in order to improve the prediction capability, especially for more viscous fluids. Their modifications showed to improve significantly the predictions of Mao's equation for low Weber, high Ohnesorge number impacts, where it previously failed within 33%. The main limitation of this approach is that it still has a strong empirical nature in the adjustment of the coefficients, which is dependent on the particular experimental conditions at which the data was obtained.

Wettability effects can be explicitly accounted in the spreading diameter by introducing the contact angle in the term of the surface energy of the spreading droplet, being the discussion focused on weather is more appropriate to use the equilibrium angle $\theta_e$, or the dynamic contact angle $\theta_d$. From the phenomenological point of view, it is recognized that the dynamic angles are more representative although good results can be obtained using the static angle, given the low velocity of the contact line at maximum extent conditions. The equilibrium contact angle is also often preferred given the difficulty in obtaining accurate measures of the dynamic contact angle.

Concerning the shape of the lamella, most models take the lamella as a flattened disk with diameter *d(t)* and height *h(t)*, so that relations between *d(t)*, *h(t)* and $D_0$ can be easily determined by mass conservation. In this context, Roisman *et al.* [35] report the incapability of energy conservation-based models to describe the flow inside the droplet, due to this simplification of the shape of the lamella. [35] compared experimental data with numerical results for the shape of the lamella and found that its thickness for sufficiently high Reynolds and Weber numbers does not depend on liquid viscosity and surface tension. Hence, an approximation for the maximum spreading could be derived out of the kinematics. In line with this, based on previous studies [30], Roisman developed a self-similar analytical solution for the viscous flow with respect to the full Navier-Stokes equation based on momentum balance [36]. Three different modes where considered to cover a wide range of possible cases in droplet impact, *e.g.* for small impact parameters We < 10 and Re < $10^2$. At the end of this analysis [36] derived the following semi-empirical expression:

$$\beta_{max} \approx 0.87.Re^{1/5} - 0.4.Re^{2/5}.We^{-1/2} \tag{13}$$

Scheller and Bousfield [37] investigated the droplet impact of Newtonian fluids onto a solid surface following an entirely empirical approach, without using energy conservation. Nevertheless, a force balance between inertial, viscous and surface tension forces is considered. Based on this analysis [37] proposed three similar expressions with general form $\beta_{max} = A.(Re^2.Oh)^b$, where *A* and *b* are fitting parameters:

$$\beta_{max} = (Re^2.Oh)^{0.123} \tag{14a}$$

$$\beta_{max} = 0.91.(Re^2.Oh)^{0.133} \tag{14b}$$

$$\beta_{max} = 0.61.(Re^2 .Oh)^{0.166} \tag{14c}$$

Detailed revision of these models can be found in Herrmann [38].

Most of the models revised up to now have a strong empirical nature, which associated to the assumptions made for the kinetic energy, viscous dissipation, wettability effects and shape of the droplet, leads to the lack of a universal description of droplet spreading. Nonetheless, the spreading of Newtonian droplets is already quite well understood, being the main issues to solve related to the interaction phenomena occurring at the liquid-solid contact line [35,37,38]. This issue is imperative to explain, particularly when interactions occur over micro-structured and/or chemically enhanced surfaces, for which wetting effects play a major role.

To close this sub-section, it is worth to briefly introduce the Attané, Girard and Morin's model (AGM model) [39], which provides the entire temporal evolution of droplet diameter, making use of a second order differential equation, based on the energy conservation principle. Despite this complex approach, [39] makes quite basic assumptions, disregarding the kinetic energy at maximum diameter extent, describing the wetting effects with the static contact angle and addressing the spreading lamella as a flattened disk, (although the authors present a long discussion on the relevance of the shape of the lamella). Attané *et al.* [39] argue that the flattened disk is actually a good approximation for the shape of the lamella, given that the viscous dissipation at the moment of impact is less relevant when compared to an adequate description of the spread factors larger than 1. This is a good approximation for impacts at low velocities and/or low viscosities, but, as shown in Roisman *et al.* [30], strong velocity gradients at the earlier stages of spreading, result in a significant viscous dissipation at moderate impact Weber numbers. Consequently, the AGM model provides more accurate predictions for low viscosity fluids at high impact velocities, when inertia and surface tension are the governing forces.

Hence, [39] allows determining the temporal evolution of the spreading diameter by solving the energy balance equation:

$$\frac{1}{12}.\frac{d}{dt}\left\{\left[\frac{2}{3}+\frac{1}{45}.\frac{1}{r^6}\right].\left(\frac{dr}{dt}\right)^2\right\}+\frac{d}{dt}.\left[r^2.(1-\cos\theta_e)+\frac{1}{3r}\right]+$$
$$+4Oh.\left[3r^4+\frac{2}{3r^2}+sr\right].\left(\frac{dr}{dt}\right)^2=0 \tag{15}$$

with the initial conditions:

$$1=\left[r_0^2.(1-\cos\theta_e)+\frac{1}{3r_0}\right]_{\theta_e<109^o} \tag{16a}$$

$$\left.\frac{dr}{dt}\right|_0 = We^{1/2}.\left[\frac{2}{3}+\frac{1}{45}.\frac{1}{r_0^6}\right]^{-1/2} \tag{16b}$$

being the free parameter:

$$s = 1.41.Oh^{-2/3} \quad (17)$$

Since Eq. (15) does not have a positive root of $r_0$ for an equilibrium contact angle of $\theta_e > 109$ it is defined to be $r_0 = 0.39$ in this case [38].

A detailed description and analysis of the AGM model may also be found in Herrmann [39].

As a comparative exercise, Figure 2 confronts the models of [32] [34] [36] [37] (only the so called free-spreading model, in Eq. 14a will be used) and [39] with our data obtained from impacts of a 3.2mm droplet of distilled water over a smooth silicon wafer surface. More detailed results on these measurements can be consulted in [39, 40]. Deviations between the experimental data can be explained by several differences in the experimental conditions and particularly in the wettability and topography of the impacting surfaces, which can significantly affect the spreading diameter. However, the disagreement between experiments and theory is also due to the empirical nature of the correlations. Most of the models deviate from our experimental data between 20-40%, exception made to the model of Roisman *et al.* [36], which deviates only 10%.

It is worth mentioning that despite the aforementioned limitations, these models already provide very satisfactory quantitative description of the spreading diameter of Newtonian droplets. In this context, after a careful description of the spreading behaviour of non-Newtonian droplets, revised in the following section, these models are revisited and adjusted, including the proper constitutive models, to evaluate their potential in predicting the spreading diameter of non-Newtonian droplets.

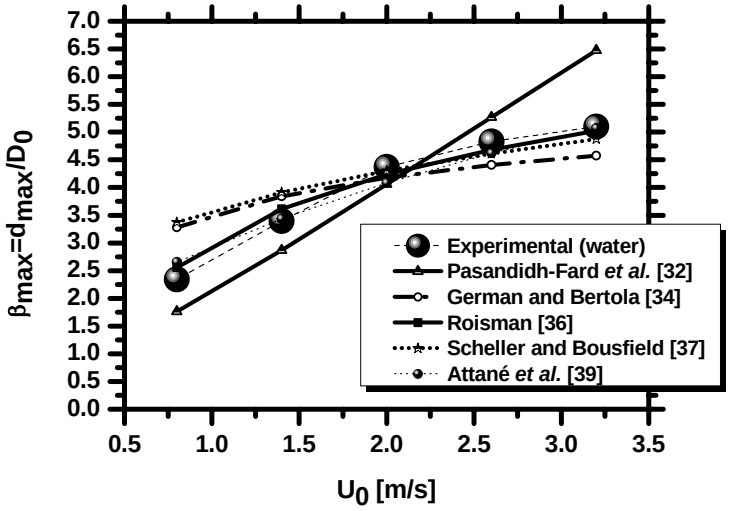


**Figure 2: Comparative analysis between various semi-empirical models for the prediction of the spreading diameter of Newtonian droplets impacting onto cold and rigid surfaces.**

## 2.3 Droplet impacts onto heated surfaces: fluid dynamics and heat transfer processes

Extensive investigation has been developed on droplet impacts onto heated surfaces within the various boiling regimes. The definition of the boiling regimes following the Nukyiama curve as illustrated in Figure 3 (i-film evaporation, ii-nucleate boiling, iii-transition and iv-film boiling) is itself a matter of investigation as it depends on the properties of the entire system, including those of the surface as, for instance surface topography, as well as on the dynamic (impact) conditions. This is particularly relevant in determining the Leidenfrost temperature, as revised for instance by Bernardin and Mudawar [41]. Hence, the heat transfer regimes for impacting droplet are

qualitatively similar to those defined in the Nukyiama curve, but significant deviations can be quantitatively observed. Numerous studies describe the morphological characteristics of the impinging droplets, many of them focusing on the spreading within the film evaporation regime and rebound within the film boiling regime (*e.g.* [31, 42-47]).

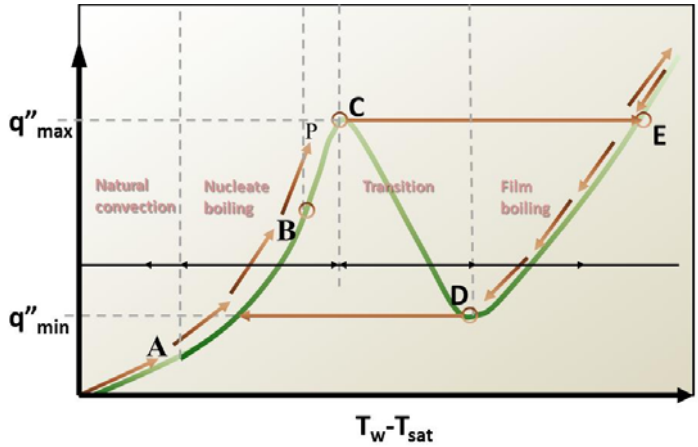


**Figure 3: Boiling curve for a liquid droplet gently deposited on a heated surface.**

Describing the heat transfer during droplet impact and spreading is quite a complex task. To simplify it many authors considered that the heat transfer between the droplet and the heated surface occurs in two stages: first the droplet spreads adiabatically until it reaches the maximum diameter and the heat transfer from the surface to the liquid only occurs afterwards. The temperature at the liquid-surface interface is considered to be constant and the heat flux from the surface to the lamella is assumed to be initially uniform. The assumption of constant liquid-surface interface temperature holds for high thermal conductivity surface materials [48,49], but not for materials with low thermal conductivity [50]. Hence the contact temperature, as defined by Seky [51] is actually vital, since it determines the rate of heat exchange between the drop and the target. However, the contact temperature defined in [50] is also a constant and uniform value. More recently, few studies address the measurements of the surface temperature, both for sessile, *e.g.* [50] and impacting drops [52–56]. Theoretical models of liquid vaporization and prediction of liquid and surface temperatures were also proposed by few authors, considering a constant and uniform liquid-solid interface temperature [57–60], most of them considering an energy balance to the system droplet-surface. A slightly different perspective is proposed by [56], although the work is more focused on predicting the heat flux.

Despite these valuable efforts, which allowed significant progress in the description of the heat transfer at droplet-surface interactions, a full consensual description has not yet been achieved. Also, many issues must still be overcome, such as the accurate description of the contact temperature, obtained at liquid-solid interface, which takes into account the heterogeneities of temperature distribution during the spreading motion. In this context, Moita *et al.* [61] proposed a new approach for the theoretical analysis of the flow and the temperature fields in a spreading droplet and in the solid substrate, based on a similarity solution of the Navier-Stokes equations, coupled with the energy equation. The solution accounts for the variation of the thermal properties of the liquids with the temperature, which have been shown by Healy *et al.* [42] to be of major importance.

The model is briefly described as follows: In the non-isothermal case the flow has to satisfy the continuity, momentum and energy equations

$$\frac{\partial \rho}{\partial t} + \nabla \cdot (\rho v) = 0 \tag{18}$$

$$\rho \frac{\partial v}{\partial t} + \rho (v \cdot \nabla) v = -\nabla \left[ p + \frac{2}{3} \mu (\nabla \cdot v) \right] + \nabla \cdot (\mu \left[ \nabla v + \nabla v^T \right]) \tag{19}$$

$$\rho C_v \left( \frac{\partial T}{\partial t} + v \cdot \nabla T \right) = \nabla \cdot (k \nabla T) \tag{20}$$

The viscosity, density, specific heat and thermal conductivity, $\mu = \mu(T)$, $\rho = \rho(T)$, $C_v = C_v(T)$, $k = k(T)$, depend on the local temperature, on the local phase and on the material. For high Weber and Reynolds numbers, the velocity field far from the wall can be described well by the remote asymptotic solution [28]:

$$u_{r0} = \frac{r}{t + \varpi} \qquad u_{z0} = -\frac{2z}{t + \varpi} + Z(T) \qquad T = T_{d0} = const. \tag{21}$$

being $T_{d0}$ the initial drop temperature and t is the time. The constant $\tau$ is determined by the initial conditions but is usually small and can be neglected for large times after impact [36].

The flow field in an incompressible spreading drop is assumed in [62] in the following form:

$$u_r = \frac{r}{t} f(\xi) \qquad T = T(\xi) \qquad u_z = -2g(\xi) \frac{\sqrt{\upsilon_0}}{\sqrt{t}} \tag{22}$$

where the self similar variable $\xi$ is defined by:

$$\xi = \frac{z}{\sqrt{\upsilon_0 t}} \tag{23}$$

$v_0$ being the drop kinematic viscosity at the initial temperature.

For convenience Roisman *et al.* [61] defined a coefficient $B_x(T)$ related to the dependence of an arbitrary material property $x$ on the temperature:

$$B_x(T) = \frac{1}{x} \frac{dx}{dT} \tag{24}$$

and re-wrote the governing equations using the self similar variable, defined in Eq. (23) in the scaled form:

$$f - g' - \frac{B_\rho}{4} (\xi + 4g') T' = 0 \tag{25a}$$

$$T'' + B_k T'^2 + \frac{Pr}{2} \frac{\upsilon_0}{\upsilon} (\xi + 4g') T' = 0 \tag{25b}$$

$$-f + f^2 - \frac{f'}{2} (\xi + 4g') - \frac{\upsilon}{\upsilon_0} (B_\mu f\ T' + f') = 0 \tag{25c}$$

where $Pr(T) = \nu C_v \rho / k$ is the local Prandtl number, $\rho$, $C_v$ and $k$ are the density, heat capacity and thermal conductivity, respectively.

Right at the surface, $\xi = 0$ the flow must satisfy the kinematic boundary conditions for the velocity and the continuity of the temperature and of the heat flux. Far from the surface, $\xi \to \infty$, the flow approaches the remote solution. These boundary conditions are:

$$f_{(\xi\to\infty)} = 1,\ T_{\xi\to\infty)} = T_{d0} \tag{26a}$$

$$T_{\xi=0_+} = T_{\xi=0_-} \equiv T_c,\ (kT')_{\xi=0_+} = (kT')_{\xi=0_-} \equiv \phi_q \sqrt{\upsilon_0 t} \tag{26b}$$

$$f_{(\xi\le 0)} = g_{(\xi\le 0)} = 0,\ T_{(\xi\to -\infty)} = T_{w0} \tag{26c}$$

Here, the contact temperature $T_c$ and the heat flux at the wall-drop interface, $\phi_q$, have to be determined from the solution of the problem.

Functions $f(\xi)$, $g(\xi)$ and $T(\xi)$ can be determined by numerical integration of the system of ordinary differential equations (25) subjected to the boundary and matching conditions (26).

The similarity solution (25)-(26) describes a flow in the spreading viscous drop, expansion of the viscous and thermal boundary layers. This is the similarity solution of the full Navier-Stokes equations which was previously reported in [36].

The solution for this set of equations in terms of the temperature distributions in both liquid and solid, for constant thermal properties of the wall materials the distribution of the wall temperature is given by:

$$T = T_c + (T_c + T_{W=})erf\left[-\sqrt{\frac{\upsilon_0 C_{vW}\rho_W}{4k_W}}\right],\ \xi \le 0 \tag{27}$$

where erf(·) is the error function, $\rho w$ $C_{vw}$ and $k_w$ are the heat capacity and thermal conductivity of the wall material, $\rho 0$ and m0 are the liquid density and kinematic viscosity, respectively, at the drop initial temperature.

The final scaled gradient of the temperature right at the interface, $T_c'$ is then obtained as the root of equation:

$$T_c'(T_c) = \frac{\sqrt{\upsilon_0}\varepsilon_W}{\sqrt{\pi}k(T_c)}(T_c - T_{W0}) \tag{28}$$

for known values of the surface effusivity, $\varepsilon_w = (\rho_w k_w C_W)^{1/2}$, of its initial temperature, $T_{w0}$, and of the dependence of the liquid thermal conductivity on temperature.

This theoretical approach was compared with experimental results for different liquid and surface material properties, as well as for different wetting conditions. As an example, Figure 4 depicts the comparison between theoretical and experimental values of the contact temperature of an ethanol droplet impacting on a smooth stainless steel surface. The droplet is initially at ambient temperature.

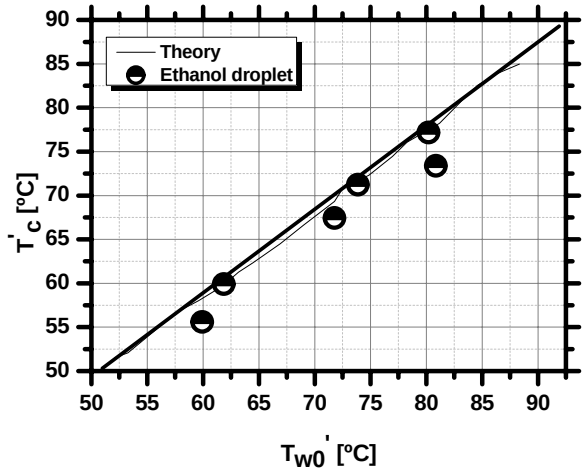


**Figure 4: Impact of an ethanol droplet with the initial temperature of 25°C impacting on a stainless steel surface (Mean roughness determined according to standard BS 1134 $R_a$=0.311μm, mean peak to valley roughness determined according to standard DIN 4768 $R_z$=2.32μm). Droplet's initial diameter is $D_0$=2.4mm and the impact velocity is $U_0$=1.3m/s. The equilibrium contact angle with ethanol is close to zero.**

The agreement is rather good, although the model is limited to time intervals relatively close to the impact instant (for a dimensionless time $t^*=tD_0/U_0<2$). Furthermore this model does not yet account for the influence of surface topography.

This effect was later addressed by other researchers, but mostly using an empirical approach.

For instance, Moita and Moreira [63] studied the impact of liquid droplets onto heated surfaces made of silicon wafers, which were micro-structured with well defined patterns. The micro-patterns were composed of square structural elements, ranging from 5μm up to 200μm. The size of the side is $l$ and height $h_R$. The pillars are apart within a distance $\lambda_R$, as defined in Figure 5.

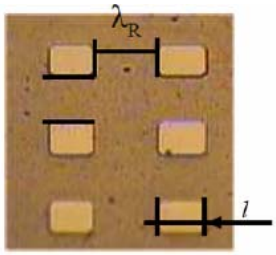


**a)**

**Figure 5: Detail of a micro-structured surface, showing the definition of the dimensions *a*, *h*, and $\lambda_R$ characterizing its topography.**

Based on a systematic variation of the geometrical parameters of the micro-patterns, the authors established an empirical relation between the roughness ratio $r_f=(2l+\lambda_R)^2/[(2l+\lambda_R)^2+8lh_R]$ with the spreading diameter, which would consequently affect the heat transferred during the spreading process. As the roughness ratio increases, the energy dissipated at the contact line within spreading also increases. Consequently, there is not a significant difference between the spreading ratio of droplets impacting on the various surfaces, as illustrated in Figure 6a). However, the recoiling process is much less evident for higher values of $r_f$ due to this dissipative effect, so that, in average, the droplet remains for a longer period over the surface, with a larger wetting area. As a

result, the heat flux becomes higher for these surfaces (Figure 6b). Here in Figure 6, the time is made non-dimensional, $t^*=tD_0/U_0$.

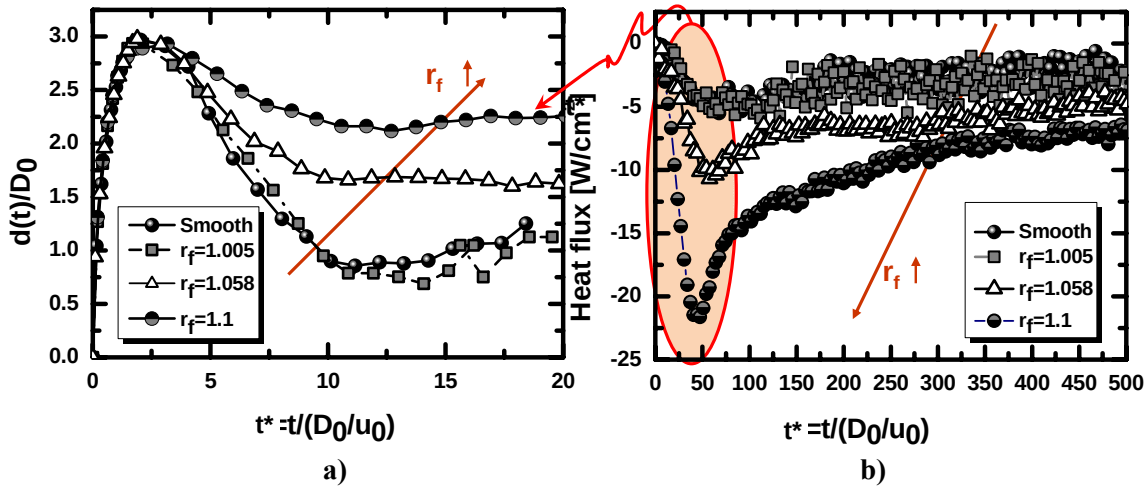


**Figure 6: Effect of the roughness ratio $r_f$ on the temporal evolution of: a) the spreading diameter for water droplets ($D_0$=3.1mm, $U_0$=1.4ms$^{-1}$) and impacting onto silicon wafers ($T_{W,0}$=120°C) and consequent effect on b) the heat flux.**

Despite these encouraging experimental results, a more detailed theoretical model is still required, which accurately accounts for the effect of surface topography on droplet-surface heat transfer.

### 2.3.1 Thermal induced atomization

When a droplet impacts the surface within the nucleate boiling regime, the lamella starts to boil at the later stages of spreading and disrupts, as the vapour pressure unbalances the equilibrium between surface tension, viscous forces and inertial forces, leading to the formation of the so-called thermal induced atomization. Size and velocity of the secondary droplets have been characterized by visualization (*e.g.* [64]) and Phase Doppler Anemometry [65,66]. Cossali *et al.* [67] combined both techniques to obtain an extended size distribution of the secondary droplets. This methodology was later developed in Moreira *et al.* [68] to be applied to impacts onto tilted surfaces. The results in [68] suggest an important role of liquid surface tension in the triggering of the thermal induced atomization. This role was later confirmed in [69], who proposes an empirical relation to predict the size of the secondary droplets resulting from thermal induced atomization within the nucleate boiling regime.

Several correlations were also proposed to predict the size of the secondary droplets within the film boiling regime, as a function of the Weber number (*e.g.* Akhtar *et al.* [65,66]), of the Reynolds number (*e.g.* Müller *et al.* [70], who also present an interesting methodology combining visualization with Particle Image Velocimetry – PIV, to obtain extended distributions of both size and velocity of the secondary droplets) or even of both (*e.g.* Moita and Moreira [69]). Better or worse agreement with each of the various proposed correlations mainly depends on the experimental conditions and on whether the governing mechanism is dominated by inertia or also has a non-negligible effect of the surface tension gradients. Hence, while the experimental results of [70] seem to be in very good agreement with a correlation solely based on the Reynolds number,

recently [71] report that the best agreement with different experimental data (including their own) was obtained with the correlation proposed in [69] for which the size of the secondary droplets is a function of both Weber and Reynolds numbers.

Extensive review on this issue can be found in [22].

## 3 Dynamic behaviour of Non-Newtonian droplets impacting onto rigid surfaces

Following the growing interest of studying droplet/wall interactions on rigid surfaces in the context of Bioengineering applications and considering that many relevant biologic fluids (e.g. blood) have shear thinning characteristics, particular emphasis is given to the dynamic behaviour and heat transfer processes occurring on shear-thinning droplets as presented in section 3.1. Then brief review on the work performed with yield-stress and viscoelastic droplets is presented in sub-sections 3.1 and 3.2, respectively

### 3.1 Dynamics of power law droplets

Most of the experimental and numerical work that has focused on the dynamic behaviour of power-law droplet impact has emphasised the spreading behaviour over cold surfaces. One of the exceptions is the work of Cheny and Walters [72], who investigated the disintegration of the Worthington jet resulting from the impact on non-Newtonian droplets on a liquid pool. Among the various classes of non-Newtonian fluids tested, [72] use a shear-thinning (Xanthan gum) solution.

The spreading behaviour of shear-thinning droplets is much similar to that of Newtonian ones, except for the acceleration and deceleration of the fluid during spreading and receding, which results in a sudden decrease and increase of the liquid viscosity, respectively. This leads to unexpected values of the spreading diameter. Hence, one of the major concerns is to accurately predict the spreading diameter of these fluids. To accomplish with this, it is vital to accurately describe the constitutive model for the non-Newtonian behaviour and include it in the droplet spreading model. In this context, one of the most interesting aspects to explore, which is directly related to the fitting parameters of the constitutive models is the effect of the concentration of the shear-thinning component in the fluid mixture. As an example, Figure 7 depicts the temporal evolution of the spreading rates for different Xanthan gum concentrations, for impacts of at two distinct velocities, over non-heated and smooth silicon wafer surface.

The $\eta_0=\mu_0/\rho$ value of the viscosity increases with growing mass fraction of the Xanthan gum, as observed on Table 1, which shows the main rheological characteristics of various Xanthan gum solutions with water. $K$ and $m=1-n$ are the parameters of the Cross model [3]. This is an expected behaviour. Hence, the spreading diameter is slightly smaller for the mixtures with larger concentration of Xanthan gum. Also, there is a slight acceleration in the spreading of the mixture with largest Xanthan gum concentration. This can be explained as follows: being more shear-thinning, the viscosity of this liquid varies faster, so overall the droplet suffers the highest viscous dissipation during the earlier stages of spreading. This is consistent with the highest $m$ and $K$ coefficients of the constitutive model. Then, as the fluid decelerates, it also becomes more viscous for the largest Xanthan concentration, contributing as well to the smaller spreading diameter obtained for the X0.35% solution. A strong damping effect is observed during the receding stage of

the droplets with highest Xanthan concentration. Hence, while the X0.05% droplets experiment an evident receding, with a substantial decrease of the diameter, a very slow receding occurs for X0.15% and X0.35% droplets and their equilibrium diameter is much larger than that of the droplets with smaller concentrations. The behaviour discussed above is more evident for impacts at higher velocities, as the velocity gradients during spreading will be higher and therefore the shear rates involved will be also higher, thus evidencing the shear-thinning nature of the mixtures with larger Xanthan concentrations.

The results depicted here are consistent with those reported by German and Bertola [73]. These authors tried to study the isolate effect of *K* and *n* parameters, although it was extremely difficult to alter one independently from the other. Nevertheless, [73] argue that as the gum concentration increases, the consistency coefficient *K* also increases (while *n* decreases) and the liquid becomes thicker, which is a dominant effect during spreading.

The results shown here are also consistent with the experimental data reported by An and Lee [74,75].

This effect of the Xanthan gum concentration (i.e. higher *K* and *m* coefficients) is actually dominant when compared to other factors such as the surface wettability, as shown in Figure 8.

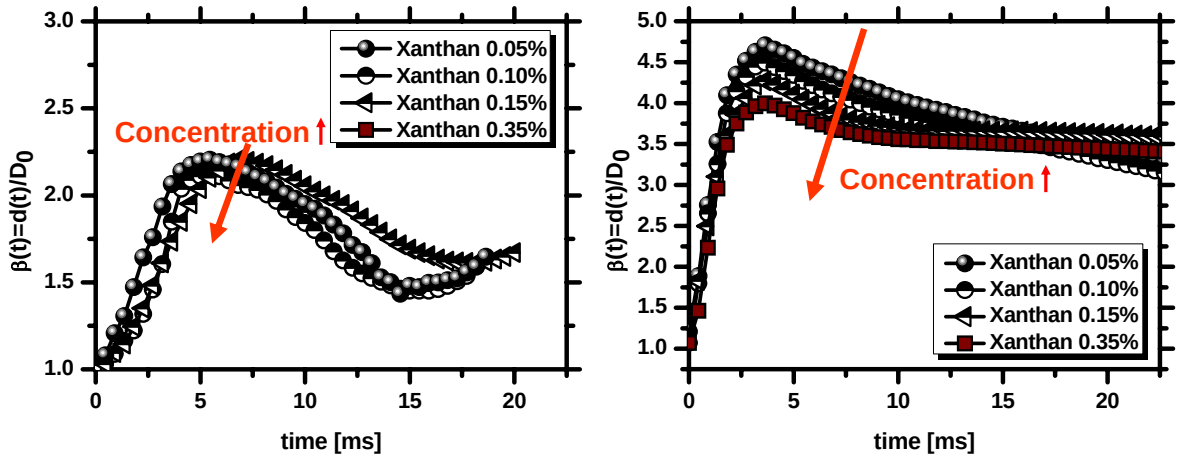


**Figure 7: Temporal evolution of the spreading rate of droplets of water+Xanthan gum solutions, impacting on a smooth silicon surface, at room temperature. a) $D_0$=3mm, $U_0$=0.8m/s, b) $D_0$=3mm, $U_0$=3.2m/s.**

**Table 1. Thermophysical properties of the working fluids taken at 20°C. Here X stands for Xanthan and the percentage following is the wt% of Xanthan gum in the mixture with water.**

| Fluid | ρ [kg/m$^3$] | $\sigma_{lv}$ [N/m]x10$^3$ | $\eta_0$ [Pa.s] | $\eta_\infty$ [Pa.s] | C [s] | m [-] |
|---|---|---|---|---|---|---|
| Water | 996 | 72.75 | 8.9x10$^{-4}$ | 8.9x10$^{-4}$ | - | - |
| X0.05% | 997 | 73.00 | 0.08 | 1.9 | 0.8 | 0.678 |
| X0.10% | 997 | 72.00 | 0.22 | 2.6 | 1.3 | 0.696 |
| X0.15% | 997 | 71.50 | 0.58 | 3.6 | 1.65 | 0.707 |
| X0.35% | 997 | 72.95 | 13.29 | 5.1 | 13.97 | 0.804 |

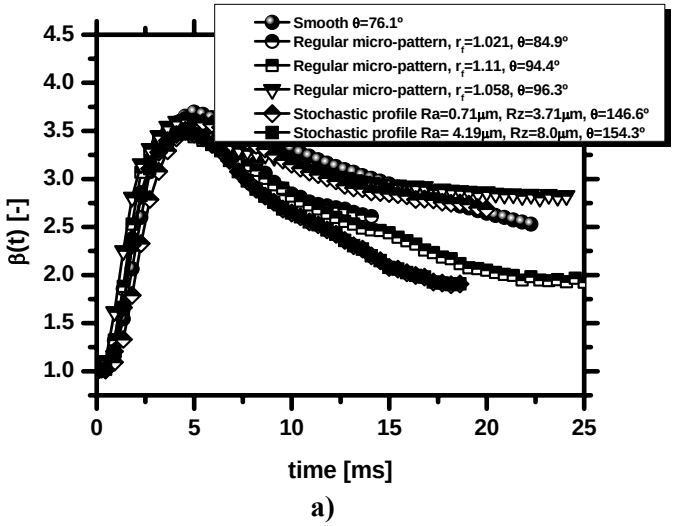


a)

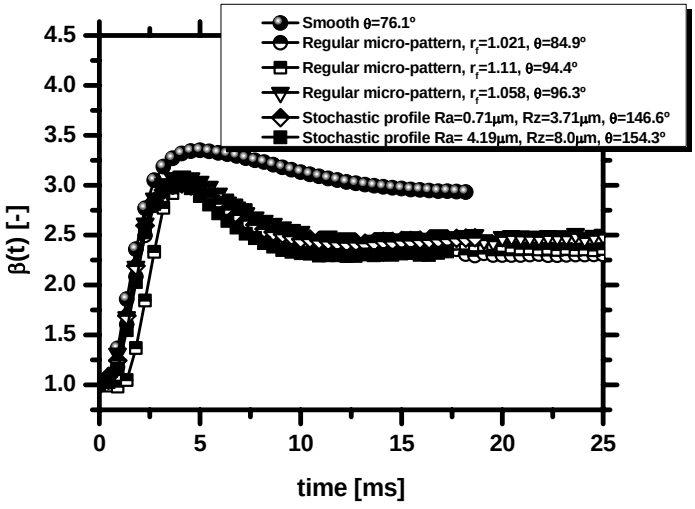


b)

**Figure 8: Effect of surface wettability on the spreading behaviour of a 3mm droplet impacting onto various cold surfaces, with $U_0$=2m/s. a) X0.05%, b) X0.35%.**

In fact, the effect of surface topography seems here quite less evident when compared to the previous results presented for Newtonian-droplets: a significant influence of the surface micro-patterning is only observed in the receding phase, for the cases in which the micro-patterning leads to a noteworthy modification of the wettability, quantified by the contact angle. This behaviour can be due to the aforementioned increase of the liquid viscosity, which in turn results in a thicker lamella. Therefore, the ratio thickness of the lamella/amplitude of the rough pillars becomes smaller and the surface is "smoother" in relation to the new effective thickness of the lamella.

To include these effects on a model, the various theoretical predictions of the spreading diameter for Newtonian droplets can be revised, by properly including the constitutive models and the dominant effects of *K* (and indirectly *n*) on the spreading behaviour, as suggested for instance by [75]. A more exhaustive investigation of spreading models is presented in Herrmann [38]. For illustrative purposes, let's consider again the formulations of Roisman *et al.* [36] and of Scheller and Bousfield [37], and define the maximum predicted spreading ratio as:

$$\beta_{max,predicted} = C_1 (Re_{eff}^2 \, Oh)^n \tag{29}$$

$$\beta_{max,predicted} = C_1 \, Re_{eff}^{1/5} - C_2 \, Re_{eff}^{2/5} \, We^{-1/2} \tag{30}$$

scaling of the thickness of the lamella, using the boundary layer thickness δ. An effective Reynolds number must be defined, $Re_{eff}=\rho U_0 D_0/\eta_{eff}$, with:

$$\eta_{eff}=\frac{\eta_0-\eta_\infty}{1+\left(C.C_3.\frac{\sqrt{\frac{\rho U_0 D_0}{\eta_{eff}}}.U}{2D_0}\right)^m}+\eta_\infty \tag{31}$$

In a different approach, one may also directly introduce the scaling of the lamella thickness *h* in the models, considering an effective viscosity, also based on the Cross model. The resulting modified formulas of [37] and [36], obtained are respectively given by:

$$\beta_{\max,predicted}=C_1\left[\left|\frac{\rho U_0 D_0}{\frac{\eta_0-\eta_\infty}{1+\left(C.C_3.\frac{3\beta_{\max}^2.U_0}{2D_0}\right)^m}+\eta_\infty}\right|.\frac{\frac{\eta_0-\eta_\infty}{1+\left(C.C_3.\frac{3\beta_{\max}^2.U_0}{2D_0}\right)^m}+\eta_\infty}{\sqrt{\rho D_0\sigma_{lv}}}\right]^n \tag{32}$$

$$\beta_{\max,predicted}=C_2\left|\frac{\rho U_0 D_0}{\frac{\eta_0-\eta_\infty}{1+\left(C.C_3.\frac{3\beta_{\max}^2.U_0}{2D_0}\right)^m}+\eta_\infty}\right|^{1/5}$$
$$-0.4.\left[\frac{\rho U_0 D_0}{\frac{\eta_0-\eta_\infty}{1+\left(C.C_3.\frac{3\beta_{\max}^2.U_0}{2D_0}\right)^m}+\eta_\infty}\right]^{2/5}.We^{-1/2} \tag{33}$$

Comparing the theoretical predictions with the experimental data, as depicted in Figure 9 one may notice a slightly better agreement between the modified Roisman relation and the experimental data. The scaling considering the boundary layer thickness provides better agreement with the experimental data for the lower concentrations, which are closer to the Newtonian droplets' behaviour. This is more noticeable at lower impact velocities. This is probably due to the geometric assumptions that are made. For such low velocities, inertia does not govern the spreading, so viscous and surface tension forces are more important and the shape of the lamella is much closer to that of a film surrounded by a disk than for a disk that is usually associated to the scaling using the thickness of the lamella *h*.

The scaling using the lamella thickness *h* seems to be more appropriate for the solutions with higher concentrations, possibly due to the larger thickness of the lamella. Nevertheless, the non-Newtonian nature of the fluids is not yet perfectly well determined since some deviations are still observed particularly for the largest Xanthan gum concentration.

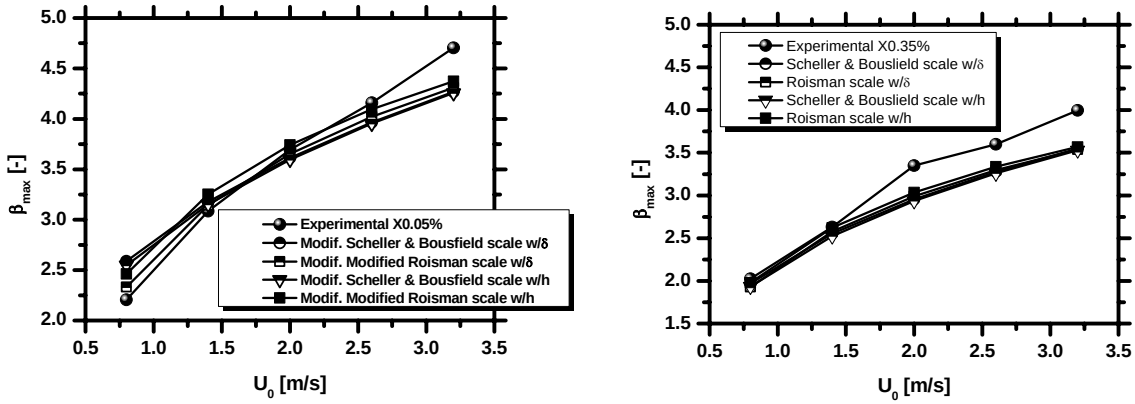


**a)** **b)**

**Figure 9: Theoretical prediction of the maximum spreading diameter vs. experimental data for: a) X0.05% solution, b) X0.35% solution.**

### 3.1.1 The effect of surface temperature

The effect of surface temperature is not dominant, while the surface temperature is kept bellow the liquid saturation temperature and the lamella does not boil. This trend can be observed in Figure 10, which depicts the temporal evolution of the spreading ratio for different values of surface temperature. Exception is made for a reduced receding velocity and equilibrium diameter when compared to those observed in for cold surfaces. This effect cannot be related to evaporation of the water since as the water evaporates, the Xanthan concentration would be higher, so the equilibrium diameter should be also larger as discussed above. Hence, these results should be attributed to rheological modifications occurring as the surface heats the liquid.

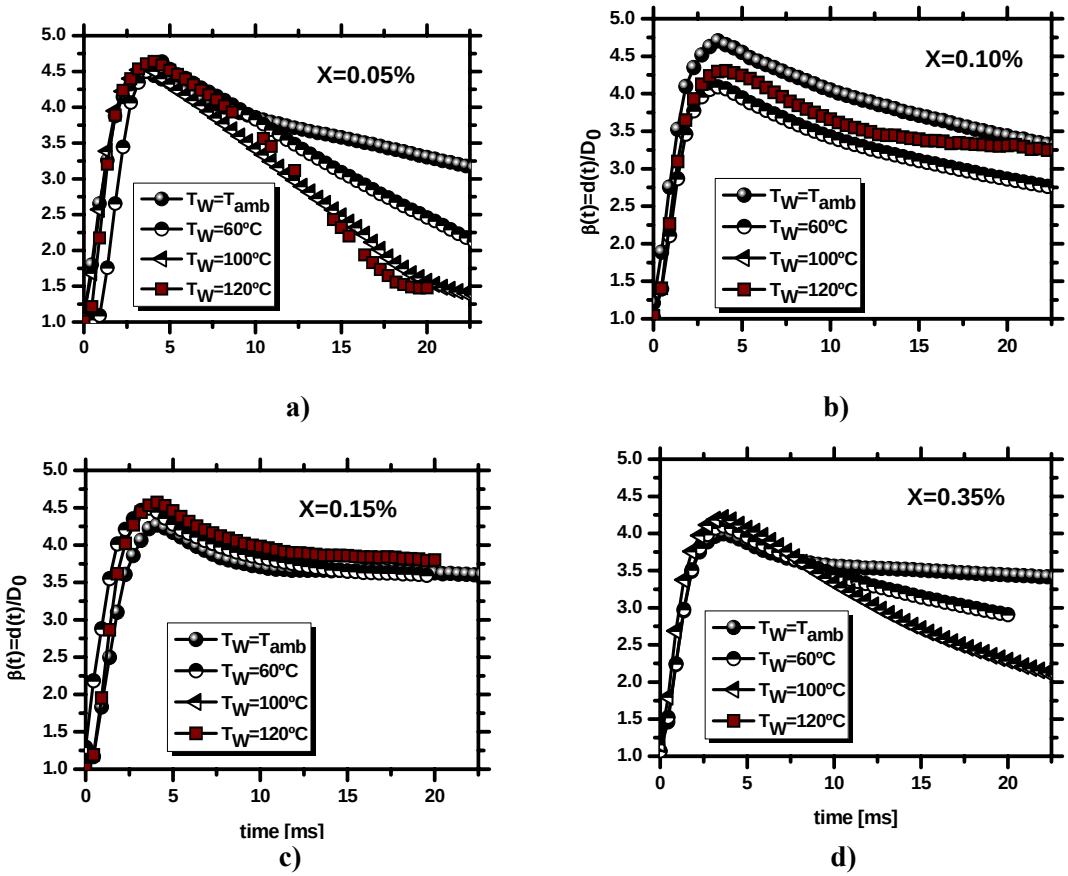


**Figure 11: Temporal evolution of the spreading rate of droplets of water+Xanthan gum solutions, impacting on a smooth silicon surface heated at various temperatures, $T_W$. The droplet is $D_0$=3mm and impacts on the surface at $U_0$=3.2m/s. a) X0.05%, b) X0.10%, c) X0.15%, d) X0.35%.**

### 3.1.2 Thermal induced atomization

The mild effect of the surface temperature on the spreading behaviour can be significantly altered as it is raised up to the saturation temperature of the liquid. For $T_W$=140ºC, the heat transfer regime falls fully within the nucleate boiling region and thermal induced atomization occurs. Visualization of droplet impacts, supported by combined image analysis and Phase Doppler measurements suggest that the secondary atomization is triggered mainly at the same time instant, regardless of the impact conditions and Xanthan concentrations, but much fewer droplets seem to be generated for higher concentrations of the Xanthan gum.

The thickness of the lamella can still be related to the effective viscosity of the lamella, but given that there is no significant change in the triggering conditions of the induced atomization, one may argue that the mechanisms of disintegration proposed by Moita and Moreira [69] to describe the thermal induced atomization occurring for Newtonian droplets are still valid here, as long as the viscosity is accurately modeled. Following this argument, one may propose that the size of the secondary droplets within the nucleate boiling regime can be given by the correlation suggested in [69]:

$$SMD / D_0 = CWe^a \, Re^b \, Ja^c \tag{34}$$

by replacing the Reynolds number was replaced by the $Re_{eff}$. $Ja=C_p(T_W-T_{sat})/h_{fg}$ is the Jakob number, being $C_p$ the heat capacity, $T_{sat}$ the saturation temperature and $h_{fg}$ the latent heat of evaporation. The fitting of the experimental data to such correlation is shown in Figure 11.

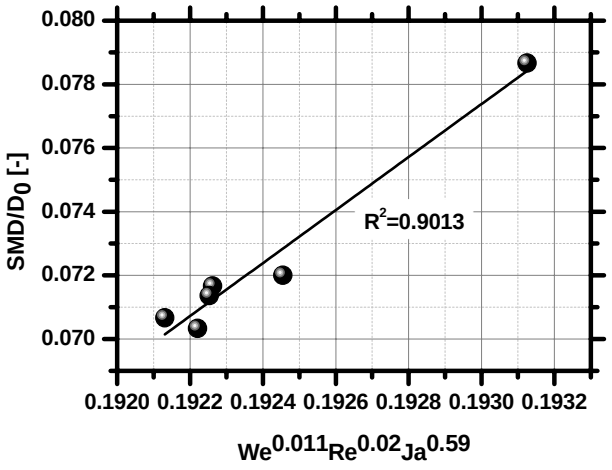


**Figure 11: Correlation for the SMD determined from the thermal induced atomization of shear-thinning droplets.**

Qualitatively, there is a good correlation, thus suggesting that the main governing parameters for the triggering of the thermal induced atomization are considered in the present correlation. However, the fitting requires a change in the exponent values, to capture what seems to be the dominating effect of the Reynolds number. This may be related to the strong variations in the shear stress which leads to significant variations of the thickness of the lamella. Hence, tuning of this correlation is still required so it can accurately capture the disintegration of the shear-thinning droplets.

### 3.2 Dynamics of yield-stress droplets

Yield-stress flows have been extensively studied for almost a century, as revised in [1] and in [6]. However, very little research has yet been done with yield-stress droplets. One interesting feature of these drops is that depending on their impact conditions, they have a very similar behaviour to that of other Newtonian and non-Newtonian fluids. For instance, [76] who studied the impact of vaseline on Plexiglass for different impact velocities, used the Cross model as a constitutive model, integrating a yield-stress component. These authors also used the Bingham number, $Bm=\tau_c D_0/\mu U_0$, where $\mu$ is defined as the zero shear rate viscosity in the Cross model.

However, [1] argues that this definition of the Bingham number is not well stood, as the Bingham number relates the viscous to the yield-stress forces and viscous dissipation only occurs during the motion of the fluid, so the term defined as $\mu$ is only valid at zero shear rate. Hence, it does not provide a good quantification of the ratio represented by Bm.

In this context, [1] defines a Bingham-capillary number, $Bm^*= \tau_c D_0/\sigma_{lv}$, which allows establishing a capillary and a viscoplastic regime. Hence, in the capillary regime $Bm^*<1$) the impact of the yield-stress droplets is similar to that of the Newtonian ones, while in the viscoplastic regime ($Bm^*>1$) a permanent deformation of the droplet (*e.g.* the oblate shape observed during droplet receding and/or rebound) occurs. These phenomena also depend on the impact conditions,

since for high Weber numbers, the impact process is dominated by inertia (and by the rheological properties), while the capillary forces naturally play a more dominant role at low Weber numbers. Despite the dissimilar behaviour observed for the various regimes, the spreading diameter is observed to be linearly dependent on the yield stress magnitude (*e.g.* [1, 73]). As for shear-thinning fluids, the effect of wettability also plays a minor role on the spreading behaviour of the yield-stress droplets [1,77].

### 3.3 Dynamics of viscoelastic droplets

As for the other classes of non-Newtonian fluids that were addressed in the previous sections, most of the research studies performed for viscoelastic droplets impacting onto rigid surfaces deals with the spreading over non-heated targets. Some analysis of the disintegration of viscoelastic droplets was performed in [78] but this is mainly the result of the impact onto a very small target. Most of the interesting findings on the studies on the impact on small targets [78,79] rendered again into the characterization of the spreading behaviour. In these studies, the spreading diameter is deduced based on an energy balance. The results also show that for impacts onto small targets, the addition of polymers leading to viscoelastic behaviour, do not affect the receding phase.

Instead, a non-negligible effect on receding was reported in [80], as the viscoelastic behaviour was related to an anti-rebound effect. While [80] associated this behaviour to the actuation of normal stresses arising near the contact line during droplet retraction, [1] further clarifies this phenomenon and shows that it is actually the result of a strong dissipative effect occurring at the contact line. This dissipative effect at the contact line was shown by visualization of fluorescent λ-DNA molecules [81]. So, in this case, it was not the study of the fluid behaviour that was used to explain the flow on biological applications, but instead a simple visualization technique commonly applied in Biology allowed to understand a complex behaviour of the viscoelastic droplets.

The impact of viscoelastic droplets is extensively reviewed in [1]. Based on the categorization of Rein [82] to establish various impact regimes for droplets impacting onto heated surfaces, (comprehensive discussion on this kind of categorizations is presented in Moreira *et al.* [22]), Bertola and Marengo [1] review the behaviour of viscoelastic droplets impacting onto heated surfaces within the nucleate and within the film boiling regimes. The results are mostly explored for the spreading mechanism, over smooth surfaces, making use of the energy balance approach.

## 4 Final Remarks

Non-Newtonian liquids are present in numerous applications. Among them, the impact of droplets on rigid surfaces is a topic of particular interest. This is a complex problem, particularly when non-Newtonian fluids are involved, due to the large spatial and temporal gradients which occur at droplet impact. Despite being studied for over a century, fluid dynamic and heat transfer processes occurring at the liquid-surface interface is still not completely described, particularly when the liquid interacts with micro-nano-enhanced surfaces. However, empirical approaches show good potential of using these modified surfaces to control the fluid motion, based on dissipative effects occurring at the contact line and enhance the heat transfer between the liquid and the surface. Unfortunately, this strategy seems to be less effective on non-Newtonian droplets, as experimental studies suggest a significantly minor effect of surface topography and wettability in

governing the dynamic behaviour of non-Newtonian droplets (for different classes of non-Newtonian fluids).

Regarding the interaction of non-Newtonian droplets with rigid surfaces, most of the experimental and numerical work performed so far has focused on the description of the spreading mechanism over smooth surfaces. The present paper shows that the approaches followed in the prediction of the spreading diameter of Newtonian droplets can be used for non-Newtonian droplet/surface interactions, as long as the constitutive model for the viscosity is appropriately introduced. Also, the scaling (*e.g.* of the dissipative term) must take into account the particular morphological features (*e.g.* thickness of the lamella) which are introduced by the different rheological properties of the non-Newtonian fluids.

A similar approach of analogy between Newtonian and non-Newtonian droplets can be used to analyse the impacts onto heated surfaces.

## 5 Acknowledgements

A.S. Moita acknowledges Fundação para a Ciência e a Tecnologia (FCT) for providing her a Post-Doc Fellowship (Ref.:SFRH/BPD/63788/2009). The author also acknowledges the contributions of D. Herrmann and of A.L.N. Moreira in the collaborative work that led to many of the results revised in the present paper.

## REFERENCES

[1] V. Bertola and M. Marengo, Single drop impacts of complex fluids: a review, Koninklijke Brill NV, Leiden, 2012, Chapter 11, 267-298.

[2] W.J. Frith, P. d'Haene and R. Buscall, Shear thinning in model suspensions of sterically stabilized particles, J. Rheol., 2005, 40, 531-548.

[3] M.M. Cross, Rheology of non-Newtonian fluids: a new flow equation for pseudoplastic systems, J. Colloid Sci., 1965, 20, 417-437.

[4] J.H. Barnes, J.F. Hutton, and K.Walters, An introduction to rheology, Elsevier Publishers, B.V., 1989.

[5] P.J. Carreau, PhD Thesis, University of Wisconsin, Madison, 1968.

[6] H.A. Barnes, The yield-stress – a review or 'παητα ρει' – everything flows?, J. Non-Newtonian Fluid Mech., 1999, 81, 133-178.

[7] P. Coussot, Rheophysics of pastes: a review of microscopic modeling approaches, Soft Matter, 2007, 3, 528-540.

[8] Q. D. Nguyen and D.V. Boger, Measuring the flow properties of yield stress fluids, Ann. Rev. Fluid. Mech., 1992, 24, 47-88.

[9] C.W. Macosko and M.S. Naser, The use of dilute solution viscosimetry to characterize the network properties of carbopol microgels, Coll. Polymer Sci, 1992, 270, 183-193.

[10] E.C. Bingham, An investigation of the laws of plastic flow, U.S. Bur. Of Standards Bull., 1916, 13, 309-353.

[11] W.H. Herschel and R. Bulkley, Konsistenzmessungen von Gummi-Benzol-Lösungen. Kolloid Z, 1926, 39, 291-300.

[12] T.C: Papanastasiou, Flows of materials with yield, J. Rheology, 1987, 31, 385-404.
[13] D.D. Joseph, Fluid dynamics of viscoelastic liquids, Springer-Verlag, New York, Berlin, Heidelberg, 2002.
[14] H. Zhu, D. De Kee and K. Frederic, A constitutive model for flow induced anisotropic behaviour of viscoelastic complex fluids, J. Non-Newtonian Fluid Mech., 2009, 157, 108-116.
[15] V. Bertola and K. Sefiane, Controlling secondary atomization during drop impact on hot surfaces by polymer additives, Phys. Fluids, 2005, 17, pp.108104.
[16] Y. Son and C. Kim, Spreading of inkjet droplet of non-Newtonian fluid on solid surfaces with controlled contact angle at low Weber number and Reynolds number, J. Non-Newtonian Fluid Mech., 2009, 162:78-87.
[17] T. Xu, J. Jin, A.C. Gregory, J.J. Hickman and T. Boland, Inkjet printing of viable mammalian cells. Biomaterials, 2006, 26, 93-99.
[18] S. Tasoglu, G. Kaynak, A.J. Szeri, U. Demirci, and M. Muradoglu, Impact of compound droplet on a flat surface: a model for single cell epitaxy, 2010, Phys. Fluids, 22, pp.082013.
[19] A.B. Robins, Non-Newtonian behaviour of dilute DNA solutions, Trans. Faraday Soc., 1964,60, 1344-1351.
[20] K. Sharma and S.V. Bhat, Non-Newtonian rheology of leukemic blood and plasma: aren and K parameters of power law model diagnostic?, Phys. Chemistry and Physics and Medical NMR, 1992, 24(4), 307-312.
[21] M. Brust, C. Schaefer, R. Doerr, L. Pan, P.E. Arratia and C. Wagner, Rheology of human blood plasma: viscoelastic versus Newtonian behaviour, Phys. Rev. Lett., 2013, 110, pp.078305.
[22] A.L.N. Moreira, A.S. Moita and M.R.O. Panão, Advances and challenges in explaining fluel spray impengment: how much of single droplet impact research is useful?, Progress Comb. Energy Sci., 2010, 36, 554-580.
[23] A.S. Moita and A.L.N. Moreira, Drop impacts onto cold and heated rigid surfaces: morphological comparisons, disinteegration limits and secondary atomization, Int. J. Heat Fluid Flow, 2007, 28(4), 735-772.
[24] R. Rioboo, C. Tropea and M. Marengo, Outcome from a drop impact on solid surfaces, Atom. and Sprays, 2001, 11, 155-165.
[25] L. Xu, W.W. Zahang and S.R. Nagel, Drop splashing onto a dry surface, Phys. Rev. Letters, 2005, 94, pp.184505.
[26] R.Y. Jepsen S.S Yoon, and B. Demosthenous, Effects of air on splashing during a droplet impact, Proc. ILASS Americas, 2006, Toronto, Canada.
[27] A.L. Yarin, Drop impact dynamics, splashing, spreading, receding, bouncing…, Annu. Rev. Fluid Mech, 2006, 38, 159-192.
[28] A.L. Yarin and D.A. Weiss, Impact of drops on solid surfaces: self-similar capillary waves and splashing as a new type of kinematic discontinuity.
[29] A.S. Moita and A.L.N. Moreira, Droplet impact on a solid surface, in:Handbook of atomization and sprays: theory and applications, Ed. Nasser Ashgriz, Springer (DOI 10.1007/978-1-4419-7264-4_8).
[30] I.V. Roisman, R. Rioboo and C. Tropea, Normal impact of a liquid drop on a dry surface: model for spreading and receding, Proc. R Soc. Lond. Ser. A, 2002, 458, 1411-1430.
[31] S. Chandra and C.T. Avedisian, On the collision of a droplet with a solid surface. Proc. Royal Soc. London A, 1991, 432, 13-41.

[32] M. Pasandideh-Fard, Y.M. Qiao, S. Chandra and J. Mostaghimi, Capillary effects during droplet impact on a solid surface. Phys. Fluids, 1996, 8(3), 650-658.
[33] T. Mao, D.C.S. Khun and H. Tran, Spread and rebound of liquid droplets upon impact on flat surfaces, AIChE J., 1997, 43, 2169-2179.
[34] G. German and V. Bertola, Review of drop impact models and validation with high viscosity Newtonian fluids, Atom. and Sprays, 2009, 19(8), 787-807.
[35] I.V. Roisman, E. Berberovic and C. Tropea, Inertia dominated drop collisions I. On the universal flow in the lamella, Phys. Fluids, 2009, 21(5), pp.052103.
[36] I.V. Roisman, Inertia dominated drop collisions II. An analytical solution of the Navier-Stokes equations for a spreading viscous film. Phys. Fluids, 2009, 21(5), pp.052104.
[37] B.L. Scheller and D.W. Bousfield, Newtonian drop impact with a solid surface, AIChe J., 1997, 41(6), 1357-1367
[38] D. Herrmann, Impact of non-Newtonian liquid droplets onto solud surfaces, Studienarbeit, Stuttgart Universitaet, 2013.
[39] P. Attané, F. Girard and V. Morin, An energy balance approach of the dynamics of drop impact on a solid surface. Phys. Fluids, 2007, 19(1), pp.012101.
[40] A.S. Moita, D. Herrmann, A.L.N. Moreira, Droplet impacts of non-Newtonian fluids for Bioengineering applications, Proceedings of the 24th ILASS-Europe 2013, Chania, Greece, 2013.
[41] J.D. Bernardin and I. Mudawar, The Leidenfrost point: experimental study and assessment of existing models, Trans. ASME, 1999, 121:894-903.
[42] W.M. Healy, J.G. Hartley and S.I. Abel-Kalik, On the validity of the adiabatic spreading assumption in droplet impact cooling, Int. J. Heat Mass Transf., 2001, 44:3869-3881.
[43] S.L. Manzello and J.C. Yang, On the collision dynamics of a water droplet containing an additive on a heated solid surface, Proc. Royal Soc. London A, 2002, 458, 2417-2444.
[44] S.L. Manzello and J.C. Yang, An experimental study of high Weber number impact of methoxy-nonafluorobutane $C_4F_9OCH_3$ (HFE7100) and n-heptane droplets on a heated solid surface, Int. J. Heat Mass Transf., 2002, 45, 3961:3971.
[45] L.H.J. Wachters and N.A.J. Westerling, The heat transfer from horizontal plate to sessile water drops in the spheroidal state, Chem. Eng. Sci., 1966, 21, 923-936.
[46] L.H.J. Wachters and N.A.J.. Westerling, The heat transfer from a hot wall to impinging water drops in the spheroidal state, Chem. Eng. Sci., 1966, 21, 1047-1056.
[47] A. Karl and A. Frohn, Experimental investigation of interaction processes between droplets and hot walls, Phys. of Fluids, 2000, 12, 785-796.
[48] K. Makino and I. Michiyoshi, The behavior of a water droplet on heated surfaces, Int. J. Heat Mass Transf., 1985, 27(5), 781-791.
[49] M. Abu-Zaid and A. Atreya, Effect of water on piloted ignition of cellulosic materials, NIST Rept., GCR-89-561, 1989.
[50] P. Tartarini, G. Lorenzini and M.R. Randi, Experimental study of water droplet boiling on hot, non porous surfaces, Heat Mass Transf., 1999, 34:437-447.
[51] M. Seki, H. Kawamura, K. Sanokawa, Transient temperature profile of a hot wall due to an impinging liquid droplet, J. hEat Transf., 1978, 100, 167-169.
[52] V.G. Labeish, Thermodynamic study of a drop impact against a heated surface, Exp. Thermal Fluid Sci., 1994, 8, 181-184.

[53] J.C. Chen and K.K Hsu, Heat transfer during liquid contact on superheated surfaces, J. Heat Transf., 1995, 117, 693–697.

[54] M. Pasandideh-Fard, S.D. Aziz, S. Chandra and J. Mostaghimi, Cooling effectiveness of a water drop impinging on a hot surface, Int. J. Heat Fluid Flow, 2001, 22, 201-210.

[55] R. Bhardwaj, J. P. Longtin and D. Attinger, Interfacial temperature measurements, high-speed visualization and finite-element simulations of droplet impact and evaportation on a solid surface, Int. J. Heat Mass Transf., 2010, 53(19), 3733-3744.

[56] G. Strotos, M. Aleksis, M. Gavaises, K. Nikas, N. Nikolopoulos and A. Theodorakakos, Non-dimensionalisation paramenters for predicting the cooling effectiveness of droplets impinging on moderate temperature solid surfaces , Int. J. Thermal Sci., 2011, 50(5), 698-711.

[57] M. Di Marzo, D. Evans, Dropwise evaporative cooling of high thermal conductivity materials, Int. J. Heat Tech., 1987, 5, 126-136.

[58] M. Di Marzo and D. Evans, Evaporation of a water droplet deposited on a hot thermal conductivity surface, ASME J. Heat Transf., 1989, 111, 210-213.

[59] M. Di Marzo, P. Tartarini, Y. Liao, D. Evans and H. Baum, Evaporative cooling due to a gently deposited droplet. Int. J. Heat Mass Transf., 1993, 36(17), 4133-4139.

[60] S. Chandra, M. Di Marzo, Y. Qiao and P. Tartarini, Effect of liquid-solid contact angle on droplet evaporation. Fire Safety J., 1996, 27, 141-158.

[61] A.S. Moita, I.V. Roisman and A.L.N. Moreira, Heat transfer during drop impact onto a heated surface, Proceedings of the ASME International Heat Transfer Conference, IHTC – 14,Washighton DC, 8-13 Agosto 2010.

[62] I.V. Roisman, On the instability of a visocus rim, J. Fluid Mech., 2010. **661**, 206-228.

[63] A.S. Moita, A.L.N. Moreira, Fom single droplet impact to micrometric droplet chains: scaling the effect of surface topography. Proceedings of the ICLASS 2012, Hedelberg, Germany, 2012.

[64] J.D. and P. Farrel, Naber, Hydrodynamics of droplet impingement on a heated surface, 1993, SAE Paper 930919.

[65] S.W. Akhtar, A.A. Nasr and A.J. Yule, Characteristics of water droplet impaction behaviour on a polished steel heated surface: Part I. Atom. Sprays, 2007, 17, 659-681.

[66] S.W. Akhtar, A.A. Nasr and A.J. Yule, Characteristics of water droplet impaction behaviour on a polished steel heated surface: Part II. Atom. Sprays, 2007, 17, 659-681.

[67] G.E. Cossali, M. Marengo and M. Santini, Secondary atomization produced by single drop vertical impacts onto heated surfaces, Exp. Thermal Fluid Sci., 2005, 29, 937-946.

[68] A.L.N. Moreira, A.S. Moita, G.E. Cossali, M. Marengo and M. Santini, Secondary atomization of water and isooctane drops impinging onto tilted heated surfaces, Exp. Fluids, 2005, 43, 297-313.

[69] A.S: Moita and A.L.N. Moreira, Development of empirical correlations to predict the secondary droplet size of impacting droplets onto heated surfaces, Exp. Fluids, 2009, 47, 755-768.

[70] A. Müller, K. Dullenkopf and H.-J. Bauer, Analysis of droplet wall interactions with graded surface roughness, Procdings of the 22nd ILASS-2008, Como Lake, Italy, 2008.

[71] P. Dunand, M. Gradeck, G. Castanet, F. LEmoine and D. Maillet, Energy balance for single or multiple droplet chains impinging onto a hot slab in the Leidenfrost regime, Proceedings of the 12th ICLASS 2012, Heidelberg, Germany, 2012.

[72] J.-M. Cheny and K. Walters, Rheological influences on the splashing experiment, J. Non-Newtonian Fluid Mech., 1999, 86, 185-210.
[73] G. German and V. Bertola, Impact of shear-thinning and yield-stress drops on solid substrates, J. Phys. Condensed Matter: an Institute of Phys. J., 2009, 21(37), pp. 375111.
[74] S.M. An and S.Y. Lee, Observation of the spreading and receding behaviour of a shear-thinning liquid drop impacting on dry solid surfaces, Exp. Thermal Fluid Sci., 2012, 37, 37-45.
[75] S.M. An and S.Y. Lee, Maximum spreading of a shear-thinnig liquid drop impacting on dry solid surfaces, Exp. Thermal Fluid Sci., 2012, 38, 140-148.
[76] S. Nigen, Experimental investigation of the impact of an (apparent) yield-stress material. Atom. and Srpays, 2005, 15, 103-117.
[77] H.A. Barnes, A review of the slip (wall depletion) of polymer solutions, emulsions and particle suspensions in viscometers: its cause, character and cure, J. Non-Newtoniam Fluid Mech., 1995, 56, 221-251.
[78] A. Rozhkov, B. Prunet-Foch and M. Vignes-Adler, Impact of water on small targets, Phys. Fluids, 2002, 14, 3485-3501.
[79] M. Vignes Adler, Physico-chemical aspects of forced wetting. In: “Drop-Surface interactions”, Edited by Martin Rein, SpringerWienNewYork, p.103, 2002.
[80] D. Bartolo, A. Boudaoud, G. Narcy and D. Bonn, Dynamics of non-Newtonian droplets, Phys. Rev. Lett., 2007, 99, pp. 174502
[81] M.I. Smith and V. Bertola, Effect of polymer aditives on the wetting of impacting droplets, Phys. Rev. Lett., 2010, 104, pp. 154502.
[82] M. Rein, Interactions between drops and hot surfaces. In: “Drop-surface interactions”, Edited by Martin Rein, SpringerWienNewYork, p. 185, 2002.